NISTIR 6701

Interferometric Metrology of Photomask Blanks: Approaches Using 633 nm Wavelength

C. J. Evans[a]
A. D. Davies [a]
R. E. Parks[b]
L-Z Shao[c]

[a]U. S. DEPARTMENT OF COMMERCE
Technology Administration
Manufacturing Metrology Division
National Institute of Standards
and Technology
Gaithersburg, MD 20899

[b]Optical Perspectives Group, Tucson, AZ

[c]Tucson Optical Research Corporation, Tucson, AZ

NIST
National Institute of Standards and Technology
Technology Administration
U.S. Department of Commerce

NISTIR 6701

Interferometric Metrology of Photomask Blanks: Approaches Using 633 nm Wavelength

C. J. Evans[a]
A. D. Davies [a]
R. E. Parks[b]
L-Z Shao[c]

[a]U. S. DEPARTMENT OF COMMERCE
Technology Administration
Manufacturing Metrology Division
National Institute of Standards
and Technology
Gaithersburg, MD 20899

[b]Optical Perspectives Group, Tucson, AZ

[c]Tucson Optical Research Corporation, Tucson, AZ

December 21, 2000

U.S. DEPARTMENT OF COMMERCE
Norman Y. Mineta, Secretary

TECHNOLOGY ADMINISTRATION
Dr. Cheryl L. Shavers, Under Secretary
of Commerce for Technology

NATIONAL INSTITUTE OF STANDARDS
AND TECHNOLOGY
Raymond G. Kammer, Director

Interferometric metrology of photomask blanks: Approaches using 633 nm wavelength illumination

C. J. Evans[*], R. E. Parks[†], L-Z. Shao[‡], and A. D. Davies[*]

Abstract

Preliminary analyses of three optical configurations for measurement of photomask blanks are described. A simple variant of the well known Ritchey-Common test should allow front surface, as-chucked flatness to be measured using current, commercially available phase measuring interferometers. Taking advantage of particular features of a special purpose interferometer installed at NIST, additional information may be obtained from two other test configurations.

Keywords: Lithography, photomasks, interferometry, scatter.

Introduction

Photomask blanks used in advanced lithography are the relatively thin parallel plates, typically made from fused silica, onto which the pattern to be replicated into photoresist is deposited. For Extreme-Ultraviolet Lithography (EUVL) masks will be reflective, comprising a patterned absorber deposited on a reflective multilayer. Out of flatness of the as-chucked mask subtracts directly from the available depth of focus (and hence process latitude) available to process engineers; hence there will be value to providing high resolution maps of the thickness variation and flatness of these blanks prior to coating. Particularly during development, there is an advantage if such measurements can be made on widely available instruments. We understand that, for the EUVL Limited Liability Corp. tolerancing[1], the flatness of the mask is assumed to be 50 nm; measurement uncertainty, therefore, needs to be some fraction of that.

Interferometric measurement of flatness is widely practiced, with state of the art uncertainties reported in the nm range. When thickness variation and homogeneity of thin transparent parallel plates are also required, the problem becomes more difficult, largely because of the long coherence length of the laser sources typically used for such measurements[2]. Classical approaches to this problem include the use of high reflectivity coatings on the front surface or anti-reflection coatings (or index matching fluids) on the rear surface to suppress the rear surface reflection. Such coatings must subsequently be removed; photomasks are sensitive to cosmetic defects and their users to contamination of their processes. An alternative to coatings is to reduce source coherence.

Some commercially available instruments effectively reduce the coherence envelope in a variety of ways. The ADE Phase Shift[§] 'Optiflat'[3], for example, uses a white light source in a Twyman-Green configuration to separate fringes from front and rear surfaces. The coherence length of the source must be less than the optical path through the sample and the sample must be placed in a

---

[*] National Institute of Standards and Technology, Manufacturing Metrology Division, Stop 8220, Gaithersburg, MD 20899-8220. Tel (301) 975-3484. E-mail: cjevans@nist.gov
[†] Optical Perspectives Group, Tucson, AZ
[‡] Tucson Optical Research Corporation, Tucson, AZ
[§] Identification of a specific commercial product does not imply that NIST endorses the product, nor that it is necessarily the best for the purpose.

specific position. Designed, apparently, for measurement of hard disk substrates, the instrument has a 100 mm diameter circular aperture. (photomask blanks are 150 mm square); adaptation of this approach could be accomplished easily, but it would be difficult for owners of current instruments to make any measurement of the part other than sub-apertures.

Zygo's MESA§ flatness tester[4] based on a dual grating system[5] uses a laser diode for illumination through a multi-mode fiber bundle to create an envelope of coherence that allows front and back surfaces to be separated. Reported repeatability[6] of 150 nm is inadequate for photomask blank metrology, although in special configurations that limit could presumably be reduced.

Tropel's "Flatmaster"[7] is an Abramson interferometer[8] which uses a coherence buster (rotating ground glass screen) in front of the laser plus a prism that generates light that is incident at a low grazing angle on the surface under test. Their 200 mm aperture instrument has a reported accuracy[7] of 100 nm, which may not be adequate for measurements of photomask blanks for next generation lithography.

In addition to the approaches described above, others have been described in the literature but are not, to these authors' knowledge, commonly available commercially. Okada et al[9] used a Twyman-Green configuration, but with a laser diode source at 795 nm wavelength. The coherence length was large enough to generate multiple interferograms. The authors accomplished wavelength shifting by modulating the drive current to the diode, took 60 interferograms, and then used a least squares fitting technique to separate surface figure from inhomogeneity.

Using a Twyman–Green configuration allows use of a very short coherence length source (as for example in Ref 3), but has disadvantages, notably that some optical components are not "common path" and hence contribute to the measured phase difference between test and reference surfaces. Schwider[10] showed that if a Fabry-Perot and a Fizeau cavity are placed in series, high contrast white light fringes are obtained from the Fizeau when separation of the Fizeau test surfaces is a rational multiple of the separation of Fabry-Perot flats. Ai[11] took advantage of the coherence properties of multimode lasers, providing high fringe visibility when the optical path difference is some multiple of the laser cavity length. Provided the optical path length of the transparent plate is not a multiple of the cavity length, the front surface can be placed in a Fizeau interferometer such that only a two-beam interference pattern is obtained. Also for Fizeau interferometers, De Groot and his colleagues have looked at various mathematical and/or multi-position approaches to deconvolving the contributions of front and back surfaces, most recently[12] through positioning the front surface at a precisely defined position with respect to the reference surface and taking advantage of the filtering characteristics of the phase shifting algorithm used; some residual contributions from the back surface are reported.

With a wavelength shifting source, the reflections between front and back surface (Haidinger fringes[13]) can be used to measure the optical path difference which combines thickness and index variations[14]. Dewa and Kulaweic[15] describe the use of an extended (low coherence) source and a tilted object to spatially separate reflections from the front and rear surfaces. A moving retro-reflector allows the reflections, individually, to be combined with the reference signal in a Twyman-Green interferometer.

The purpose of this report is to describe interferometric measurements of photomask blanks that could be made at the National Institute of Standards and Technology (NIST) using existing equipment without the use of coatings which must subsequently be removed. The first major section describes the use of a Ritchey-Common configuration using a conventional, commercially

available phase measuring interferometer. The second section discusses a flatness measurement that may be made using a custom-built interferometer (XCALIBIR) at NIST. The final section considers how that same interferometer might be used to detect and localize small cosmetic defects.

Ritchey-Common test

The Ritchey-Common test[16] allows the interferometric measurement of a flat using a spherical wavefront. Its implementation on a modern, Fizeau phase measuring interferometer (PMI) is easily understood by reference to Figure 1. A transmission sphere generates, beyond focus, a diverging beam into which the test flat is placed at an appropriate angle. The wavefront continues to diverge beyond the tilted flat until it reflects off a concave spherical surface and retraces its path into the interferometer imaging system (Measurement 2). The optical path difference introduced by deviations h of the flat is $2h \cos a$, where a is a function of position on the part; this variation of sensitivity with position can easily be compensated in post-processing of phase data. In a separate measurement (Measurement 1), the return sphere is measured directly with the transmission sphere to allow separation of the surface departure of the flat from the errors of the interferometer, transmission sphere, and return sphere. The details of those calibration techniques will not be discussed here[17],[18]. Suffice it to say that a measurement of relatively low uncertainty[19] can be made of a flat of larger aperture than the commercially available PMI being used, although further analysis will be needed to address set-up issues. In particular, if a circular flat is the aperture stop in a Ritchey-Common test, a quadratic term (power) in the tilted flat is distinguishable from incorrect spacing of the return sphere since it adds an astigmatic component[18]; for a square stop (tilted), there will presumably be a term with interesting symmetries about both vertical and horizontal axes.

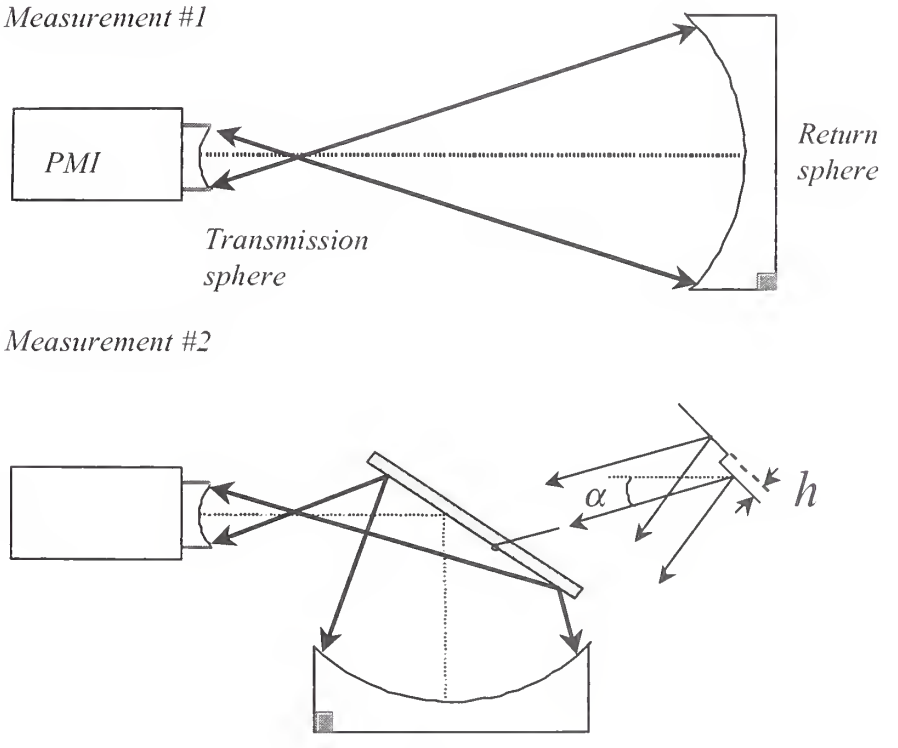

Figure 1

In the case of a transparent flat (photomask blank), coherent reflections are possible from both front and back surfaces of the flat. Figure 2 shows the case (for a very small beam divergence and a glass of index 1) where the part of the beam returning from the concave spherical mirror reflects off the back surface of the plate, forming a focus that is displaced from the focus of the light returning into the interferometer. This shift is determined by the thickness of the plate; for the highly simplified case of Figure 2, this "stray" light can be prevented from returning into the interferometer using an appropriately placed beam block or "stop". Note that this places a limit on the f-number of the transmission sphere that may be used since there are shifts both along and transverse to the original optical axis of the interferometer. In addition to the stray reflection shown in Figure 2, two other unwanted reflections can arise; rays reflecting off the rear surface on its way toward the return sphere and then the front surface (rear-front) and twice from the rear surface (rear-rear)

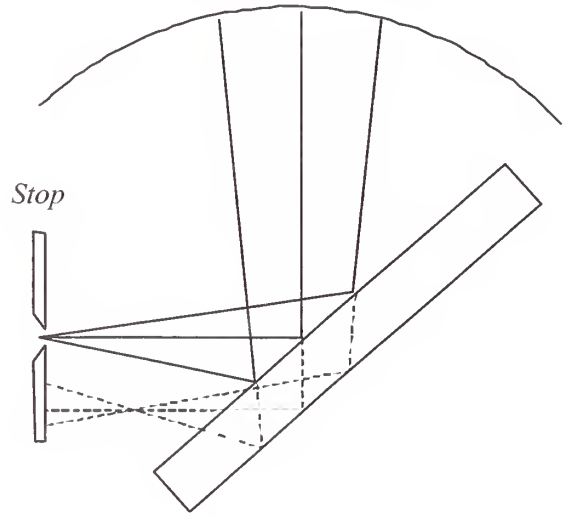

Figure 2

For real glasses (n > 1) rays reflected off the rear surface will be refracted as they traverse the front surface, producing an aberrated wavefront with a focus displaced somewhat from the idealized position discussed above. The imperfect wavefront from the interferometer adds further aberrations. To test if these stray reflections can be eliminated by a beam blocking stop, a system using a 150 mm nominal aperture commercially available f/3.2 transmission sphere and 6.25 mm thick fused quartz mask blanks has been modeled using Zemax§ optical design code. Figure 3 shows the overall layout, Figure 4 a close up of the photomask and Figure 5 a close-up of the focii, which are separated laterally by approximately 4.4 mm. For the f/3.2 cone, axial shift is clearly not a problem. A similar lateral separation is predicted for the rear-front reflections, and about twice that for rear-rear. The spot diagram (generated using the Zemax image analysis option) indicates that even for the rear-rear case, the aberrated spot (Figure 6) should not be so large as to be impossible to remove with a stop. Thus it appears that stray light should not be a problem for this measurement configuration.

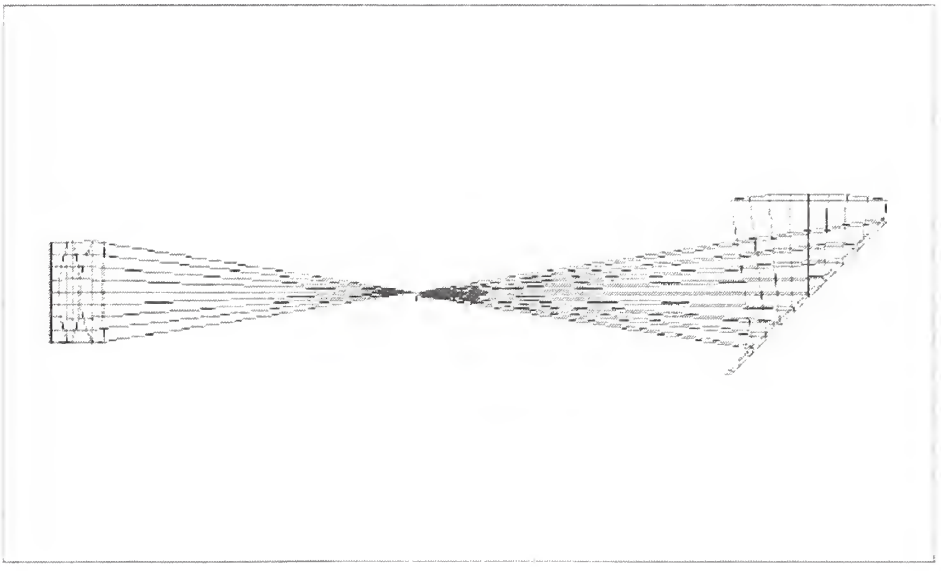

Figure 3

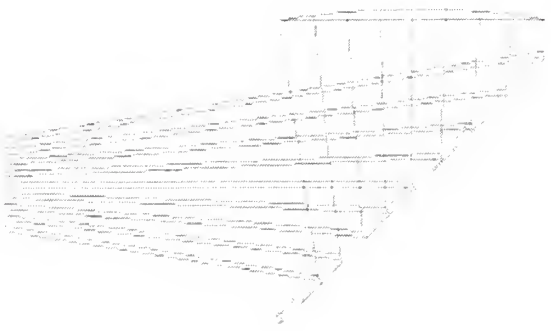

Figure 4

Figure 5

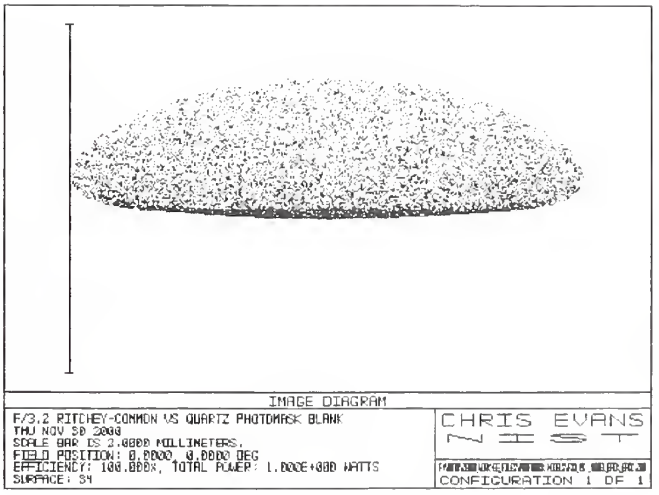

Figure 6 (scale bar is 2 mm)

A practical issue with the test configuration is reflectivity and fringe contrast. The photomask surface will have ~4% reflectivity, as does the reference surface of the transmission sphere. A highly reflective (aluminized) return sphere must be used (assumed reflectivity of 95%). The modulation, or fringe visibility, γ, is given by[20]:

$$\gamma = \frac{2A_r A_t}{(A_r^2 + A_t^2)} = 0.073$$

where A_r and A_t are the wavefront amplitudes in the reference (i.e. from the transmission sphere) and test or return beams. Note that the default modulation threshold for at least one commercially available PMI[21] is 0.07. Reflectivity is a function of incident angle and polarization; since the test is double pass, a doubling of the reflectivity will lead to 4 times the amplitude in the test arm and hence nearly that increase in fringe visibility. If necessary, fringe visibility could be improved dramatically by adding a not very efficient anti-reflection coating to the reference surface of the transmission sphere; this, however, would exacerbate problems when trying to make the calibration measurements on the highly reflective sphere.

Photomask flatness measurements on XCALIBIR

NIST has recently installed a custom built 300 mm aperture interferometer, known by the acronym XCALIBIR (Figure 7). This instrument is designed to be flexible, having a large number of possible set-ups, including the use of HeNe laser or diode sources, both operating at a wavelength of 633 nm; the latter allows variation of the coherence length. Fizeau and Twyman-Green configurations are possible. The 300 mm aperture allows direct measurement of photomask blanks with a plane wave, provided the other issues discussed earlier can be resolved.

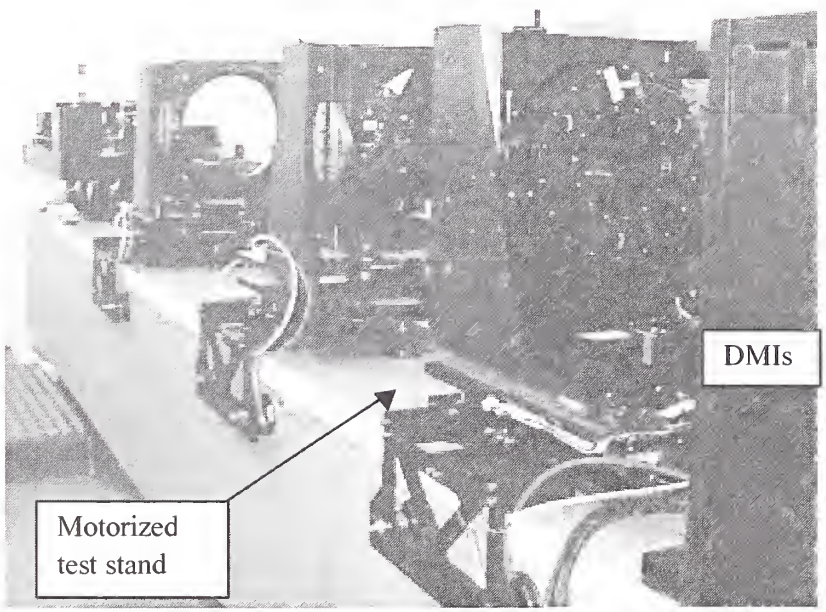

Figure 7

Figure 8 shows both a schematic arrangement and the results of a preliminary experiment performed on XCALIBIR using the diode source running with a short coherence length. The

system was set up with about 5 vertical tilt fringes, and intensity profiles through those fringes taken as the optical path difference between the two legs of the interferometer was deliberately changed. Clearly, fringe visibility decreases dramatically above 10 mm OPD, showing some ringing between approximately 15 and 20 mm and then decreasing again. The optical path difference between front and back surface modulations will be $2nt$, where n is the index and t the thickness. It is not essential that measurements be made at the peak of fringe visibility; hence for photomask measurements it should be relatively straightforward to adjust the reference or test arm length (in a Twyman-Green configuration) such that light reflected from the rear surface simply adds background, incoherent intensity to the interferogram. An appropriate configuration for testing a photomask blank (provided it is sufficiently flat that the interferogram from any surface is within the dynamic range of the interferometer) is shown in Figure 9.

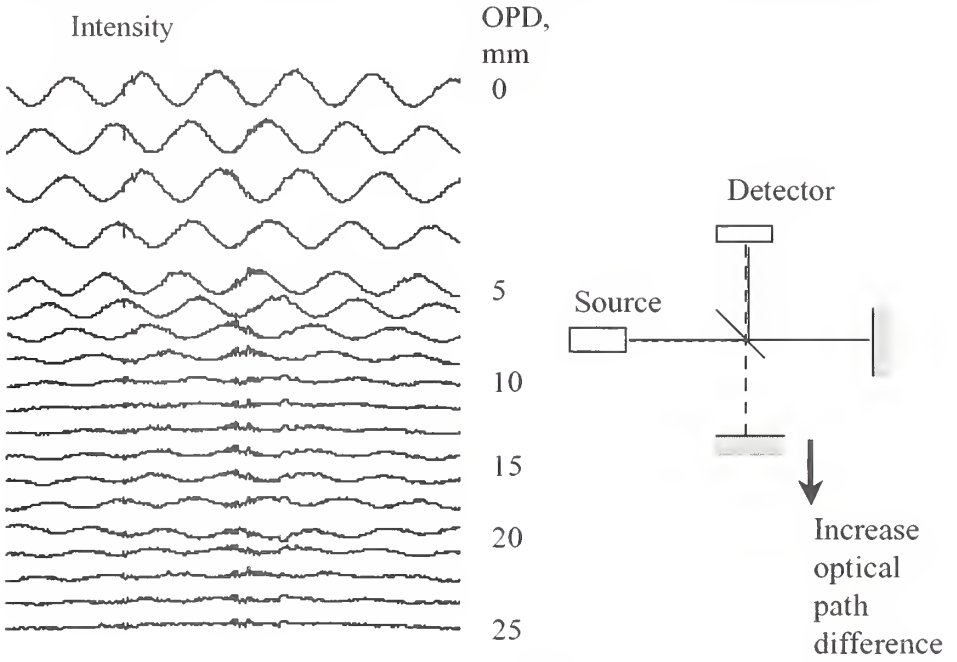

Figure 8

Note that XCALIBIR has a remotely operated motorized test stand (Figure 7); hence we can obtain not only the front surface flatness, but thickness variation by applying an obvious variant of Schwider et al's method for homogeneity testing[22]. The first measurement (W1) is of the front surface reflection. Now move the test stand until the rear surface reflection is obtained (W2). Next the stand is moved again until an interferogram is obtained from the reflection of the return mirror (W3). In addition a fourth measurement (W4) is needed without the photomask in place. According to Schwider et al, provided the index variation is small compared to the mean refractive index, the thickness variation, ?t is given by:

$$? t = 1/2((W2-W1)-(W3-W4))$$

Index variation data (homogeneity/striae) can also be obtained.

Since the part is moved between set-ups (and tilt removed from each measurement) it is not normally possible to deduce the linear term (eg wedge between surfaces). On XCALIBIR, however, motion of the stage can be measured by 3 displacement measuring interferometers, thus offering enough additional information to deduce wedge and/or linear variations in index.

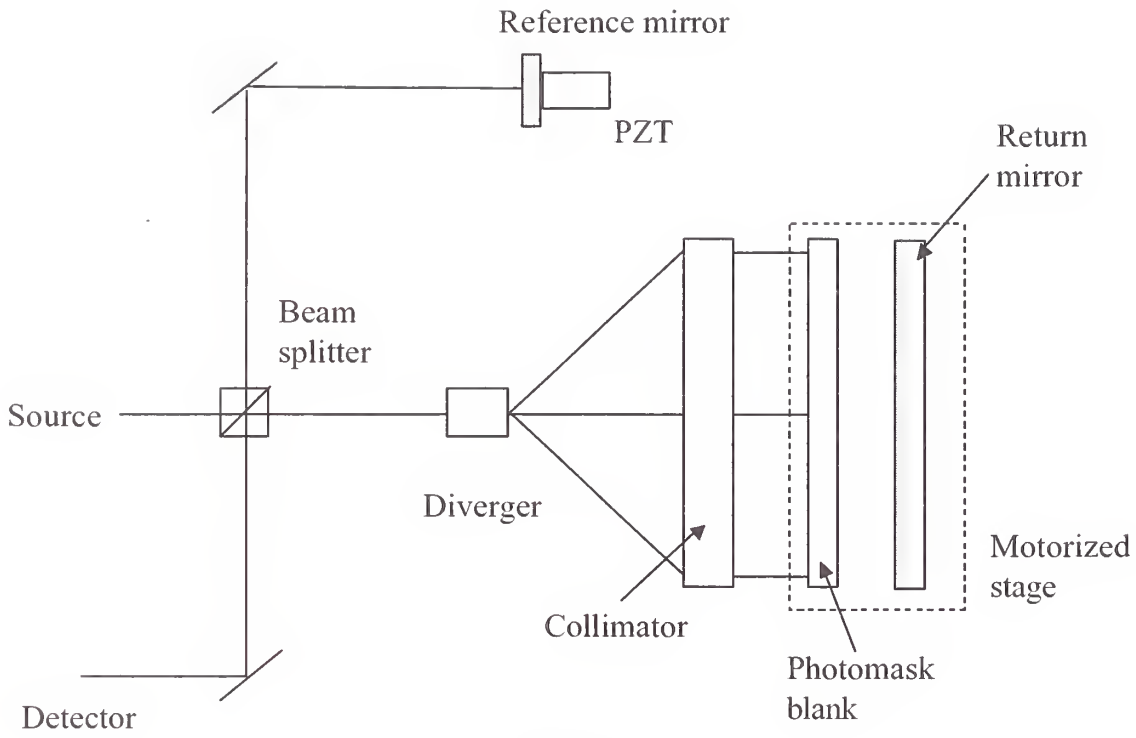

Figure 9

In addition to the freeform flatness measurements discussed above (which assumes a simple edge support for the photomask blank), as-chucked flatness measurements could also be made. We have not yet demonstrated precision measurement of flats on XCALIBIR using the diode source; the design goals for the instrument, however, were for much smaller uncertainties that those needed for photomask blanks.

Defect detection

Solar coronagraphs use occulting discs to block out the direct light from the sun's photosphere, thereby permitting observation of the faint light of the sun's outer corona. Work at NIST[23] in the early 1990's applied the same idea to figure measuring interferometers, blocking the image of the test and reference surfaces with a small central obscuration and allowing the near angle scattered light to be imaged onto the interferometer's detector. This work drew on the ideas embodied in current systems for detecting and characterizing wafer defects; light scattering locates the defects in the coordinate system of the wafer. Given the location of the defect in part coordinates, its topography or chemistry, for example, can subsequently be investigated using other instruments which may have a small field of view and high resolution.

Figure 10 is a paraxial model of XCALIBIR in Twyman-Green mode with the reference leg shutter closed. Clearly a stop could be placed conveniently at the focus in the imaging system. Placing a 0.1 mm diameter beam stop in the model shows that a tilt of only 0.003 degrees is required for the light to clear the stop. This implies that, if we consider it as an angled facet, a 200 nm wide, 0.1 Angstrom deep defect will scatter light past the stop. Clearly such issues as detector sensitivity and stray light control will have to be addressed; in addition, the actual imaging system will perform differently from the paraxial model, requiring additional effort to

optimize stop size. Experimentally, a series of chrome dots of various sizes could be deposited onto an appropriate glass substrate, which would likely be tilted and anti-reflection coated.

The earlier NIST work showed that it was necessary to perform a differential measurement. Specifically, the system collects scattered light from every surface. For convenience, consider the intensity detected at the camera, I(x,y) as the sum of the intensities scattered by the system and by the photomask:

$$I_1(x,y) = I_s(x,y) + I_p(x,y)$$

Taking a second measurement where the photomask is displaced mechanically by a distance ? x gives:

$$I_2(x,y) = I_s(x,y) + I_p(x+?x,y)$$

The difference between these intensity images contains a double image of any scatterer on the photomask plus variations in source intensity, camera noise, etc. A variety of image processing algorithms may be used to identify (in detector coordinates which will map directly to part coordinates) these scatter sites[24]. Further work will also be required to ascertain if the intensity and/or size (on the detector) offers sufficient information to make accept/reject decisions without further inspection

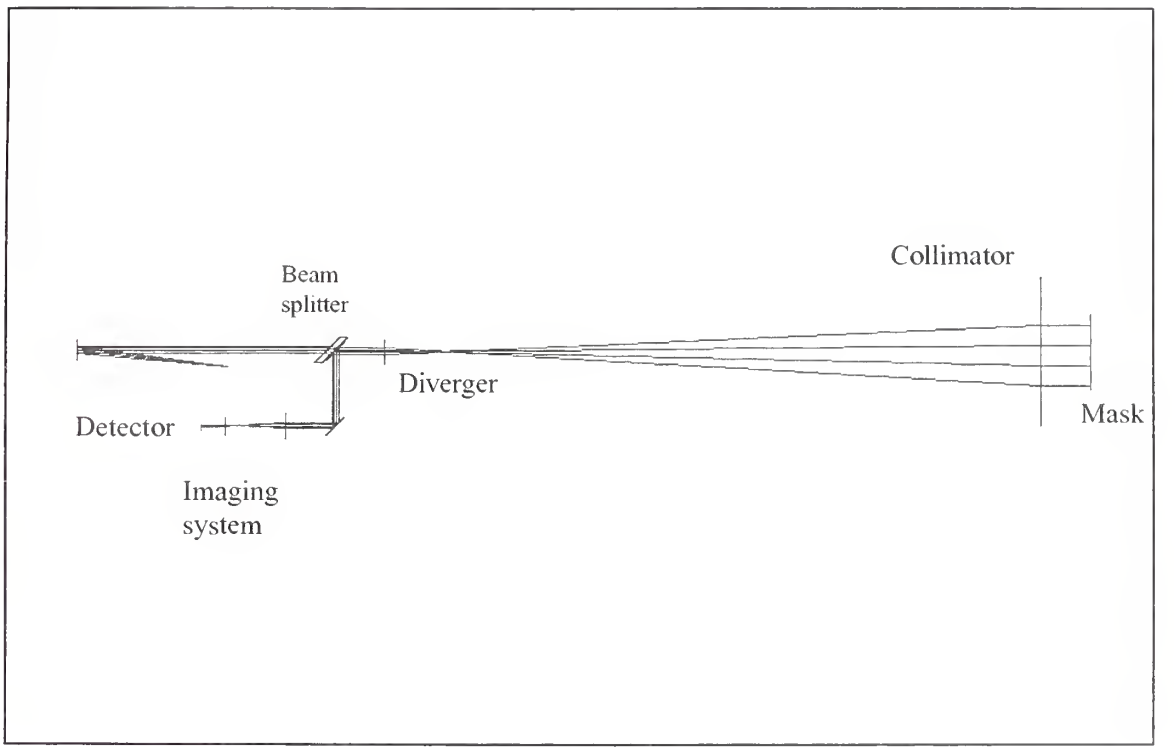

Figure 10

Concluding remarks

This report has discussed techniques which may be used to measure photomask blank flatness and/or thickness variation to uncertainty levels appropriate for EUV lithography. These methods

are based on existing equipment installed at NIST, as is a method for detecting defects. Each method requires additional analytical and experimental work to evaluate its performance.

Two of the methods described make use of XCALIBIR, although neither requires all the capabilities of that instrument. Special purpose instruments embodying the basic ideas could easily be built if needed.

Acknowledgements

CE thanks Ken Blaedel (Lawrence Livermore National Laboratory) for stimulating him to think again about the problem of how to measure thin parallel plates interferometrically. Thanks are also due to Peter de Groot (Zygo Corporation) and Tyler Estler (NIST) for their helpful comments on the draft manuscript.

References

[1] Blaedel K. Personal communication with CE, October 2000
[2] Schwider J. Partially coherent illumination in interferometers for optical testing" OSA 1998 Technical Digest Series, No 12 "Optical Fabrication and Testing" pp164-6
[3] http://www.phase-shift.com/optiflat.shtml
[4] http://www.zygo.com/
[5] de Groot P. J. "Grating interferometer for flatness testing" Optics Letters, 21(3) 228-30 (1996)
[6] de Groot P, Deck L., and Colonna de Lega C. "Adjustable coherence depth in a geometrically desensitized interferometer" SPIE 1998 Annual Meeting paper # 3479-02
[7] http://www.tropel.com/html/spec_fm200.htm
[8] Abramson N. "The Interferoscope: a new type of interferometer with variable fringe separation" Optik (Stuttgart) 30, 56-71 (1969)
[9] Okada K., Sakuta H., Ose T. and Tsujiuchi J. "Separate measurements of surface shapes and refractive index inhomogeneity of an optical element using tunable-source phase shifting interferometry" Applied Optics, 29(22) 3280-85 (1990)
[10] Schwider J. "White light interferometer" Applied Optics, 36(7) 1433-7 (1997)
[11] Ai C. "Multimode laser Fizeau interferometer for measuring the surface of a thin transparent plate" Applied Optics, 36(31) 8135-8 (1997)
[12] de Groot P. "Measurement of transparent plates with wavelength-tuned phase-shifting interferometry" Applied Optics, 39(16) pp2658-63 (2000)
[13] Mantravadi M. V. "Newton, Fizeau and Haidinger interferometers' in Optical Shop Testing, 2nd Ed (ed D. Malacara) Wiley, 1992
[14] Kulawiec; A. W "Interferometer for measuring thickness variations of semiconductor wafers " US Patent 5,909,282 (1999)
[15] Dewa P. G. and Kulawiec; A. W. "Grazing incidence interferometry for measuring transparent plane-parallel plates" US Patent 5,923,425 (1999)
[16] Ritchey G. W "On the Modern Reflecting Telescope and the Making and Testing of Optical Mirrors" Smithson. Contrib. Knowl., Vol 34, No 3, (1904) as quoted by Ojeda-Castenada J. in "Focault, Wire and Phase Modulation Techniques", Chapter 9 of Optical Shop Testing (ed D. Malacara),1st edition, Wiley, 1978.
[17] Shu K. L. "Ray-trace Analysis and Data Reduction Methods for the Ritchey-Common Test" Applied Optics, Vol 22 (12), pp1879-86, (1983)
[18] Parks R. E., Evans C. J. and Shao L-Z. "Implementation of the Ritchey-Common test for 300 mm wafers" " OSA 1998 Technical Digest Series, No 12 "Optical Fabrication and Testing" pp104-7
[19] Parks R. E., Shao L-Z., and Evans C. "Absolute Ritchey-Common test for circular flats" OSA 1996 Technical Digest Series, No 7 "Optical Fabrication and Testing" 24-7
[20] Bruning J. H. "Fringe Scanning Interferometers" in 'Optical Shop Testing', (D. Malacara, ed), First edition, pp409-437, Wiley, 1978

[21] WYKO 6000

[22] Schwider J., Burow R., Elssner K.-E., Spolaczyk R., and Grzanna J. "Homogeneity testing by phase sampling interferometry" Applied Optics, 24(18) 3059-61 (1985)

[23] Sullivan P., Evans C. and Parks R. "Improved measurement of the topography of high precision optics" OF&T Workshop, Boston, June 1994

[24] Sullivan P. J. "Interferometer bandwidth expanded by software" Laser Focus World, October 1995, p35